Marine Geophysical Research (2022) 43:23
https://doi.org/10.1007/s11001-022-09483-z

ORIGINAL RESEARCH PAPER

Check for updates

Seismic sequence stratigraphy and depositional evolution of the Cretaceous-Paleogene sedimentary successions in the offshore Taranaki Basin, New Zealand: implications for hydrocarbon exploration

Mahmoud Leila[1] · Islam El-Sheikh[2] · Ahmed Abdelmaksoud[3,4] · Ahmed A. Radwan[2]

Received: 15 September 2021 / Accepted: 2 May 2022 / Published online: 6 June 2022

Abstract

The seismic stratigraphy and sedimentary facies of the Cretaceous and Paleogene sedimentary successions in north-eastern offshore part of Taranaki Basin, New Zealand have been investigated in order to unravel their depositional evolution and identify the potential hydrocarbon plays. Interpretation of regional seismic lines covering the entire shelf-slope and deep-water regions as well as integrating seismic and sedimentary facies allows the identification of several seismic-stratigraphic sequences within the studied successions. Early Cretaceous syn-rift successions (C1 sequence) were deposited in the structural lows near the present-day slope as swamp and marsh facies changing basinwards into turbidites and marine shales. The post-rift Cretaceous sequences (C2, C3 sequences) started with the progradation of the Taranaki delta (C2A-C2D units) followed by sedimentation of the transgressive C3A-E facies accumulated in response to thermal subsidence and high-rates of clastic supply. Extensive shelf conditions prevailed during the deposition of C2 and C3 Cretaceous sequences continued during the Paleogene with deposition of uniform marine shales throughout the basin. Rates of sediment supply substantially decreased during Oligocene prompting the deposition of marine micrite-rich carbonate. Variation in fossil content confirms the occurrence of several cycles of sea level fluctuations and episodic variations in terrigenous input. Organic-rich facies could be associated with the prograding clinoforms of the C2B unit and probably contain, basinward, large amount of gas and oil prone kerogen. The transgressive facies of C2D unit may also contain organic-rich shales basinward and coal near the present day Taranaki shelf. Potential reservoirs are hosted on the C3 transgressive estuarine sandstones. Paleogene mudstones are excellent regional seals for the hydrocarbons generated and trapped in the underlying Late Cretaceous facies.

Keywords Taranaki Basin · Seismic stratigraphy · Biostratigraphy · Sedimentary facies · Cretaceous · Paleogene

Introduction

The Taranaki Basin is a huge sedimentary basin accommodating up to 11 km thick Cretaceous and younger sedimentary clastic wedge lying beneath New Zealand's western continental margin (Fig. 1). It is one of the largest adjoining, interconnected Cretaceous-Cenozoic sedimentary basins and covers an area of about 100,000 km^2 (King and Thrasher 1996; Ainsworth and van der Pal 2004; Giba et al. 2010; King et al. 2011; Reilly et al. 2015; Radwan et al. 2021, 2022; Radwan and Nabawy 2022). Taranaki Basin is the most petroliferous hydrocarbon province in New Zealand containing large gas (7 TCF) and oil reserves (500 MBBL) (e.g. Giba et al. 2010; King et al. 2011; Higgs et al. 2012; Strogen et al. 2014). Most of these commercial petroleum

✉ Mahmoud Leila
mahmoud_lotfy@mans.edu.eg

1 Geology Department, Faculty of Science, Mansoura University, Mansoura, Egypt

2 Department of Geology, Faculty of Science, Al-Azhar University, Assiut Branch, Assiut 71524, Egypt

3 Department of Earth Sciences, Khalifa University, 127788 Abu Dhabi, United Arab Emirates

4 Department of Geology, Faculty of Science, Assiut University, Assiut 71516, Egypt

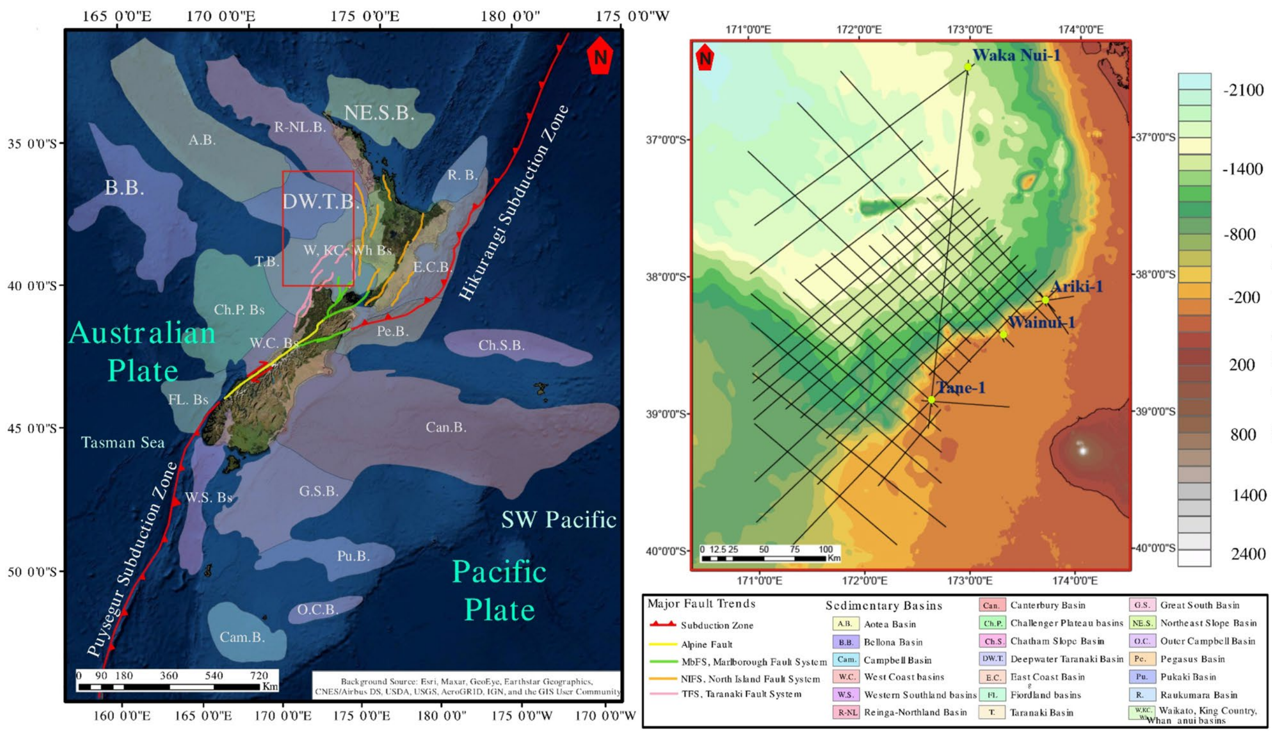

Fig. 1 **A** A map showing the location and bathymetry of the study area in the northeastern offshore part of Taranaki Basin, New Zealand; **B** red rectangle shows the location of the studied seismic survey and wells in the framework of the general setting of New Zealand. Bathymetry data were acquired from Ryan et al. (2009)

reserves are contained in the Cretaceous and Paleogene successions which host the most prospective source rocks and reservoir intervals (e.g. Uruski et al. 2003; King et al. 2011; Radwan et al. 2021, 2022).

The opening of Taranaki Basin accounts for Gondwana breakup and separation between Zealandia, Antarctica and Australia. This was accompanied by accumulation of thick syn- and post-rift Cretaceous and Paleogene-Neogene sedimentary successions above the pre-rift Jurassic metasediments and pre-Cambrian basement (Carter 1988; Mortimer et al. 2014; Strogen et al. 2017). The Gondwana break-up and the key elements of the Zealandia Cretaceous-Paleogene rifting phase have been widely discussed over the last decades (Laird 1993; Turnbull et al. 1993; King and Thrasher 1996; King et al. 2011; Strogen et al. 2017). However, little is known about the factors controlling the infill of such huge basin with sediments through geological time.

The onset of the Cretaceous-Paleogene rifting phase has been estimated as early as 105 Ma, however, it was likely commenced later in Taranaki region (70–80 Ma; Laird 1993; Cook et al. 1999; Laird and Bradshaw 2004). Strogen et al (2017) proposed a two-phase Cretaceous-Paleogene rifting in the Taranaki region producing series of NW, WNW and NE extensional normal faults associated with half grabens. The basin response to these rifting phases and the subsequent evolution of the Cretaceous-Paleogene syn- and post-rift sedimentary successions have gained little interest. Here we present the results of a basin-scale integrated study, comprising regional 2D seismic reflection profiles, biostratigraphy and sedimentology data worked out, in order to reconstruct the basin evolution during the Cretaceous and Paleogene times and to discuss some implications for hydrocarbon exploration.

Geologic setting

The composite geological evolution and the complex morphological setting of the Taranaki Basin, comprising diverse superimposed sub-basins, uplifted areas and depocenters, were both resulted from several tectonic events that have been taken place in Zealandia microcontinent from Middle-Cretaceous to Recent (Laird 1992, 1993; King and Thrasher 1996; Norvick et al. 2001; Laird and Bradshaw 2004). The basin's sedimentary cover represents the record of both the Zealandia rifting phase during Gondwana break-up and the Paleogene plate boundary processes (King and Thrasher 1996; Uruski et al. 2003; Nicol et al. 2005; King et al. 2011; Strogen et al. 2017). Taranaki Basin lies on the Zealandia continental crust along the eastern margin of Gondwana. The basin evolution and its structural elements were controlled by the kinematics of the Australian and Pacific plate boundaries prevailed during the Late Cretaceous-Paleocene and Oligocene-Neogene times. The main tectonic elements present within the basin include: rift-related transform faults, passive margin, platform subsidence linked to incipient subduction, foreland basin and subduction-related transform faults, as well as volcanic arc, fold-thrust belt, and back-arc rift. The Oligocene-Neogene plate boundary deformation only impacts the southern and eastern regions of the Taranaki Basin, whereas the western parts remained relatively undeformed (e.g. Uruski et al. 2003; Nicol et al. 2007). The Oligocene-Neogene Pacific-Australian plate convergence largely overprinted the elements of the former tectonic phases in the Taranaki Basin (King 2000; Uruski et al. 2003; Kamp et al. 2004; Reilly et al. 2015).

Deposition in Taranaki basin started with the sedimentation of Middle Cretaceous strata inside the half grabens above the Paleozoic–Mesozoic basement terranes (King et al. 2011). This initial deposition was followed by four major phases of sedimentation resulting in accumulation of the long-lived Late Cretaceous, Paleogene and Neogene sequences throughout Zealandia (Isaac et al. 1994; King et al. 2011; Mortimer et al. 2014 and references therein). The first phase includes the deposition of the Late Cretaceous and Paleocene syn-rift transgressive facies (Fig. 2). During the Eocene, control of rift physiography on sedimentation started to be negligible and the basin was completely submerged by marine water. Therefore, Eocene post-rift transgressive marine facies and fine-grained terrigenous sediments covered the entire Taranaki Basin. Renewed tectonic subsidence during Oligocene marks the onset of the third phase when the basin was largely submerged with deposition of deep-water carbonate (Uruski et al. 2003; King et al. 2011). A prolonged marine regression took place during the Neogene contemporaneous with a progradation of the Taranaki continental shelf and accumulation of mixed marine and terrigenous facies (Fig. 2).

Data and methods

The present study is based on an integrated subsurface dataset including seismic and well data from the north-western offshore sector of Taranaki Basin (Fig. 1). The data used in this study has been kindly provided by the New Zealand Ministry of business, innovation and employment (MBIE) and institute of geological and nuclear Sciences (GNS). A total of 37 2D time-migrated post-stacked reflection seismic profiles covering an area of approximately 800 km^2 were utilized in this study. The seismic survey has been acquired by TGS-NOPEC and GNS Science in 2001 and processed to Pre- Stack Time Migration (PSTM) by Western-Geco in early 2002. This survey was acquired with a 6000 m-long streamer, a 4000 cubic inch air gun array, and was recorded to 8 s two-way seismic travel-time (twt). No. of channels are 480 and shot interval is 25 m and 60 fold. The seismic data were interpreted using Schlumberger Petrel 2017 software. Well data includes wireline logs (gamma ray, sonic, resistivity, density and neutron), core photographs and core reports that have been acquired by GNS Science and were provided with permission from the Ministry of economic development, New Zealand. Seismic data was calibrated with well-stratigraphic horizons using time check shots. Different depositional trends were identified using the gamma ray motifs and patterns. Upward variation in gamma ray values often reflect changes in lithofacies and hence the depositional environment (e.g. Rider and Rider 2002; Nazeer et al. 2016; Abdelmaksoud et al. 2019; Ali et al. 2020a, b; Yasser et al. 2021; Leila et al. 2022; Abdelmaksoud and Radwan 2022). Relative ages of the different stratigraphic horizons were identified using the available biostratigraphic data. The biostratigraphic dataset from the core and cutting reports has been re-evaluated and compared to the seismic facies for a better understanding of the evolution of basin-fill sedimentary successions. The available core photos were analysed in order to identify the different sedimentary lithofacies that were then grouped into facies associations. The sedimentary facies associations and biostratigraphic results (e.g. benthonic, planktonic forams and palynology) aided in the identification of the depositional environment of the different stratigraphic sequences.

Results and interpretation

Seismic stratigraphy

Early cretaceous

The Cretaceous sedimentary strata in the Taranaki deepwater were accumulated unconformably above the older Jurassic beds and basement rocks in the half-grabens as syn-rift megasequences (Figs. 3 and 4). Jurassic strata are scattered and preserved only in the deepest parts of the basin corresponding to the depocenter of the half-graben structures (Fig. 3; TGS-NOPEC 2001). The seismic facies corresponding to the Jurassic strata consist of low-amplitude, semi-transparent and chaotic reflections displaying a notable increase in seismic amplitude upward. Jurassic and lower Cretaceous sediments were likely accumulated during the onset of the rifting phase that was associated with a phase of active subsidence in the back arc basins that were initially developped at the Gondwana margin (Uruski et al. 2003; Uruski and Baillie 2004). The seismic facies of the Early Cretaceous sequence (C1) vary greatly throughout the basin; they are almost absent near the shoreline and the thickness increases significantly basinwards. C1 facies pinches-out toward the shelf and therefore C1 sediments are not encountered in the drilled shallow-water wells. Near the slope, C1

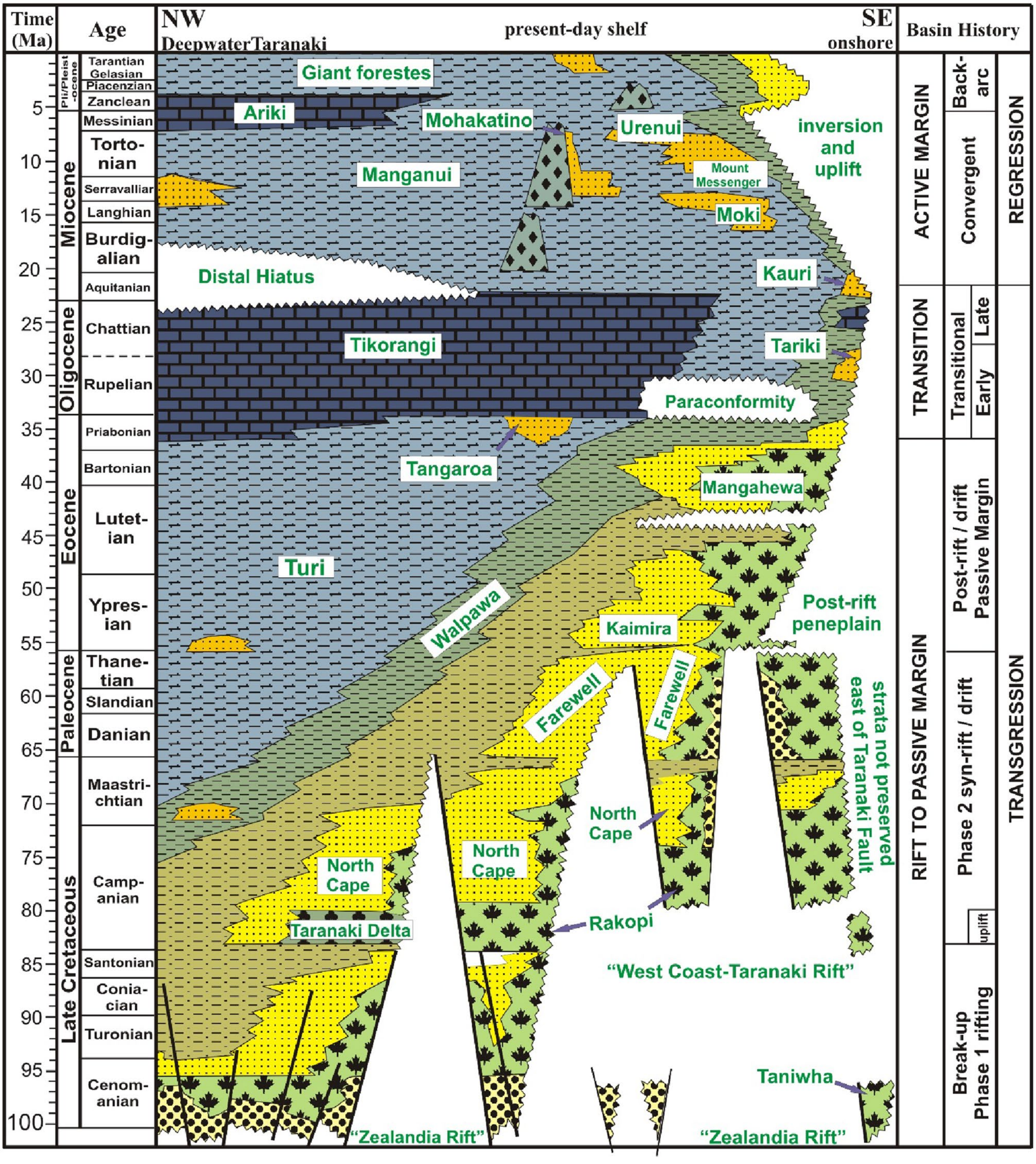

Fig. 2 Generalized lithostratigraphic chart of the Taranaki Basin showing the main lithostratigraphic units (King and Thrasher 1996; Strogen et al. 2014)

includes low-amplitude, low-frequency, disorganized and semi-chaotic reflections often onlapping the small depressions and small fault-controlled channels (Fig. 5A, B). Basinwards, C1 seismic facies changes into parallel, continuous, vertically-variable amplitude and frequency reflections. Near the slope, the C1 sedimentary successions are represented by fluvial coarse-grained clastics near the shoreline locally derived from the fault scarps. In the depocenters of the half grabens, swamp and marsh sediments were likely accumulated (e.g. Uruski et al. 2003). In Taranaki deep-water, the

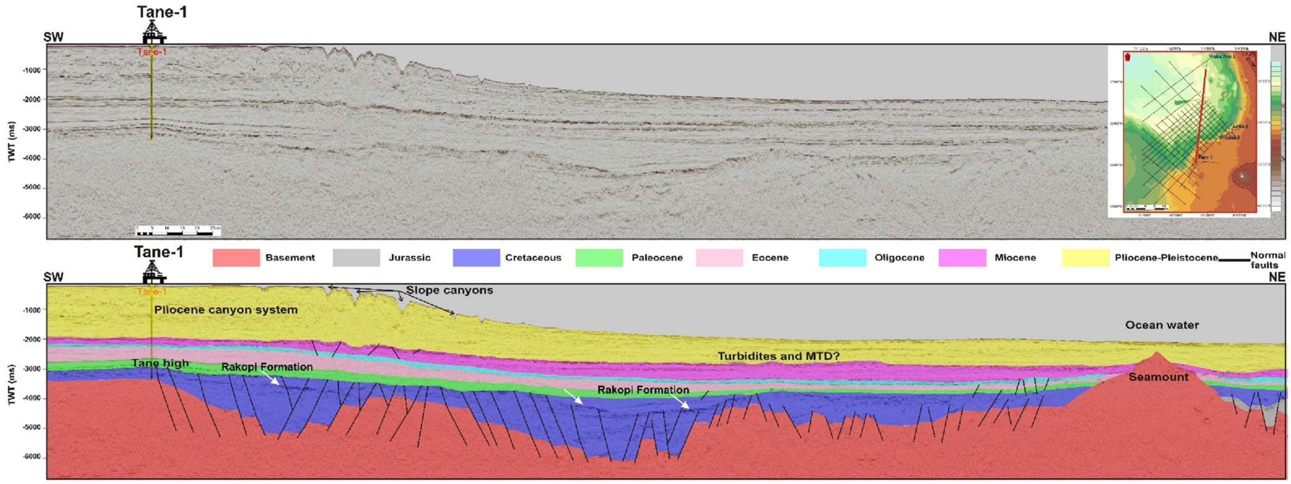

Fig. 3 Interpreted regional seismic profile normal to the trend of the Deepwater Taranaki Basin showing the main seismic horizons and stratigraphic successions hosted in the basin

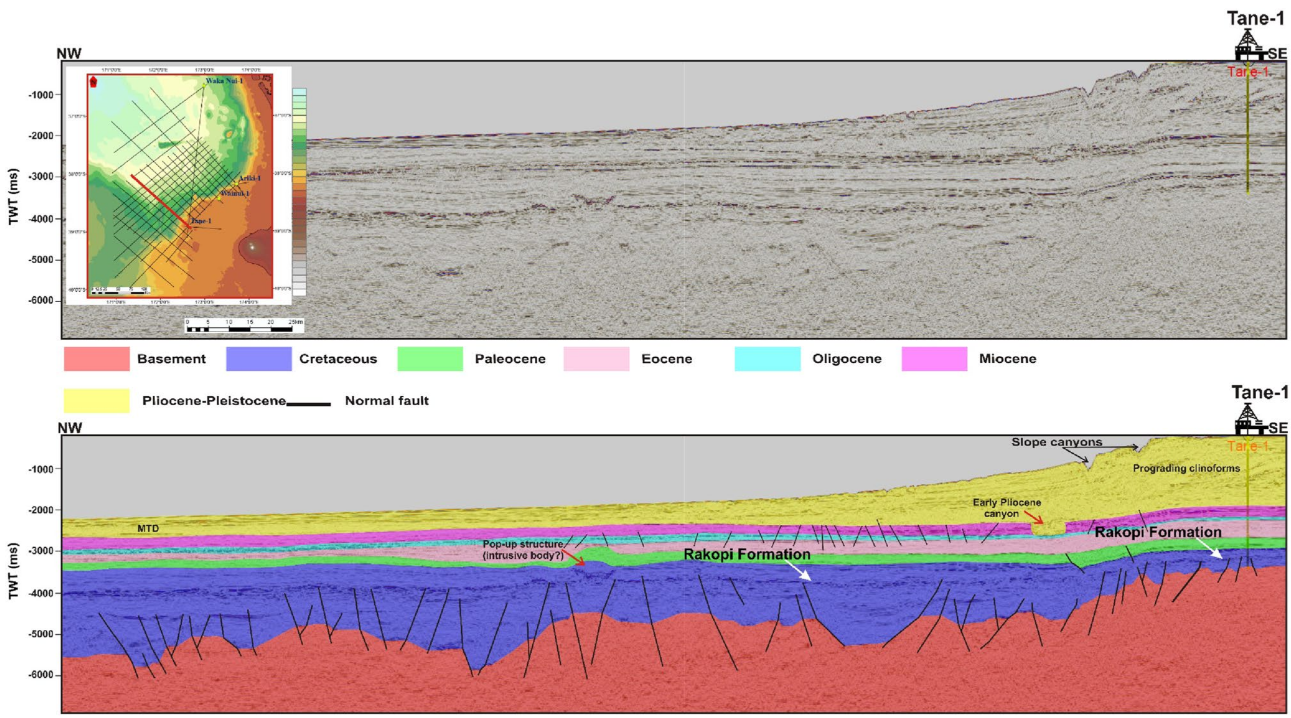

Fig. 4 Interpreted regional seismic profile normal to the trend of the Deepwater Taranaki Basin and passing through Tane-1 well showing the different seismic horizons and seismic-stratigraphic units

sediments of C1 succession change into chaotic turbidites and marine facies (Fig. 5C, D).

Late cretaceous

In Taranaki deep water, the onset of Upper Cretaceous sedimentation started with the deposition of the Taranaki delta megasequence (C2) (Uruski and Baillie 2004; Kroger et al. 2017). The boundary between C1 and C2 megasequences is very sharp and probably regflects a period of erosion and/or non-deposition. C2 megasequence comprises four second-order sequences (C2A-C2D) recording successive episodes of relative sea level rises and falls (TGS-NOPEC 2001). C2A is the oldest sequence and coincides with the earliest phase of the Taranaki delta progradation during the sea level highstand. C2A consists of low-amplitude prograding

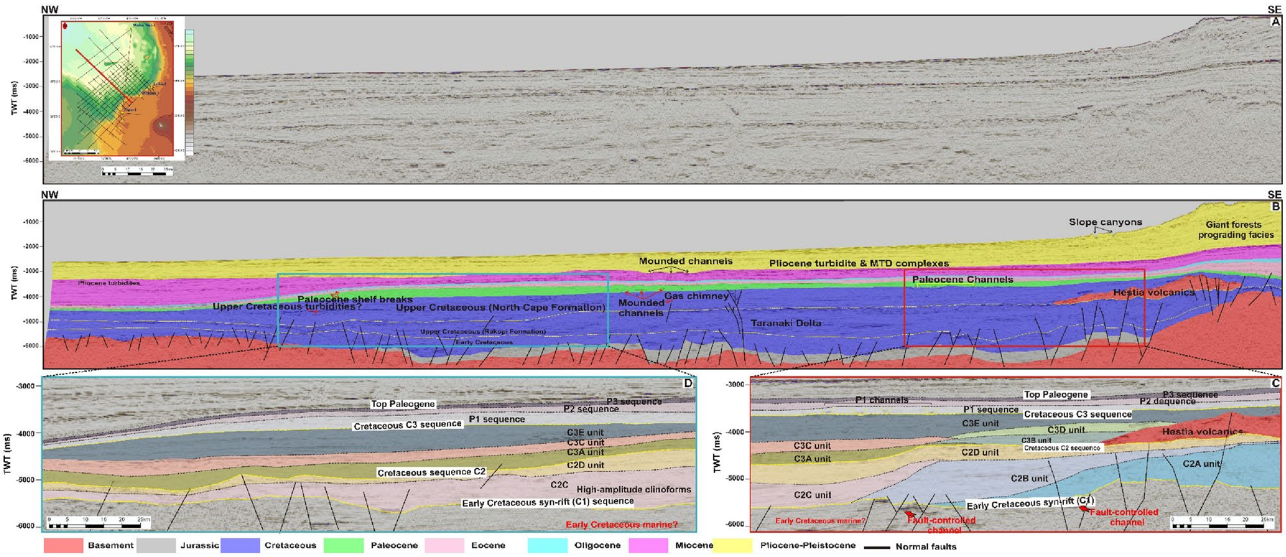

Fig. 5 Interpreted regional seismic profile normal to the present-day shore-line and passing across the Wainui-1 well illustrating a basinward variation in the seismic-stratigraphic units. Enlarged sections clarifies the seismic facies, reflector terminations and geometry of the different seismic-stratigraphic units

clinoforms terminating against the fault-block highs near the shelf edge. The maximum thickness of C2A is recorded (~ 700 ms two way time “ms TWT”) near the slope and pinches-out basinwards (Fig. 5C, D).

C2B sequence is more extensive basinwards, it onlaps C2A and comprises medium to high-amplitude clinoforms downlap onto the underlying syn- and pre-rift facies. C2B sediments are transgressive clastic facies accumulated during the sea level rise. C2B sequence pinches-out basinwards where it attains a maximum thickness of ~ 550 ms TWT. C2C represents the lowstand wedge sediments that are only observed in the deep water regions. C2C seismic facies is represented by parallel, high-amplitude and reflectivity reflections onlapping the C2B facies and downlap onto the C1 syn-rift facies. C2C unit thickens basinwards with a maximum of ~ 500 ms TWT and pinches out landward. The sediments of C2B and C2C sequences are not encountered in any of the studied wells, however, the seismic facies point to uniform, fine-grained clastic facies probably deposited in deep marine conditions (e.g. Uruski et al. 2003; King et al. 2011).

The deposition of C2C lowstand wedge was terminated by a regional sea level rise and transgressive event which marks the deposition of C2D sequence (TGS-NOPEC 2001). C2D facies comprise semi-continuous, parallel, high-amplitude reflections that are extensively distributed in both deep and shallow water regions. C2D sequence attains a maximum thickness of ~ 600 ms TWT in the slope and pinches out both basinward and near the shelf. In Tane-1 well, the sediments of C2D sequence are represented by the shales alternated with coal and marine sandstones of the Rakopi. In Wainui-1 and Ariki-1 wells, the sediments of C2 sequence are completely absent and Rakopi Formation was not deposited (Fig. 6).

A sea level lowstand prevailed after the deposition of the C2D facies which are onlapped by lowstand systems tract sediments that marks the base of the transgressive megasequence C3 presenting the latest Cretaceous facies in Taranaki deep-water. The extensive shelf area formed during the deposition of Taranaki Delta (C2 sequence) lasted during the deposition of C3 sediments that followed the same depositional pattern of C2 megasequence with no signs of major changes in the basin physiography. The C3A is a lowstand sequence followed by four transgressive successions (C3B-C3E, Fig. 5C, D). The C3A seismic facies includes discontinuous vertically variable amplitude and frequency reflections downlapping onto the underlying C2D facies. C3A unit is localized in the deep water regions attaining maximum thickness of ~ 250 ms TWT near the basin-floor and pinches out toward the shelf. The seismic characteristics of C3A facies reveal that they most likely represent the sediments of a lowstand clastic wedge deposited near the basinfloor.

The sediments of C3B unit are more extensive than that of C3A and is more developed near the present-day Taranaki Shelf where it attains a maximum thickness of ~ 750 ms TWT. C3B pinches out basinward where it downlaps the C3A facies. The seismic facies of C3B comprises continuous, high-amplitude, and high-reflectivity reflections near the shelf changing into low-amplitude semi-transparent facies basinwards. C3C constitutes a wedge-shaped unit of vertically-variable amplitude reflections localized near

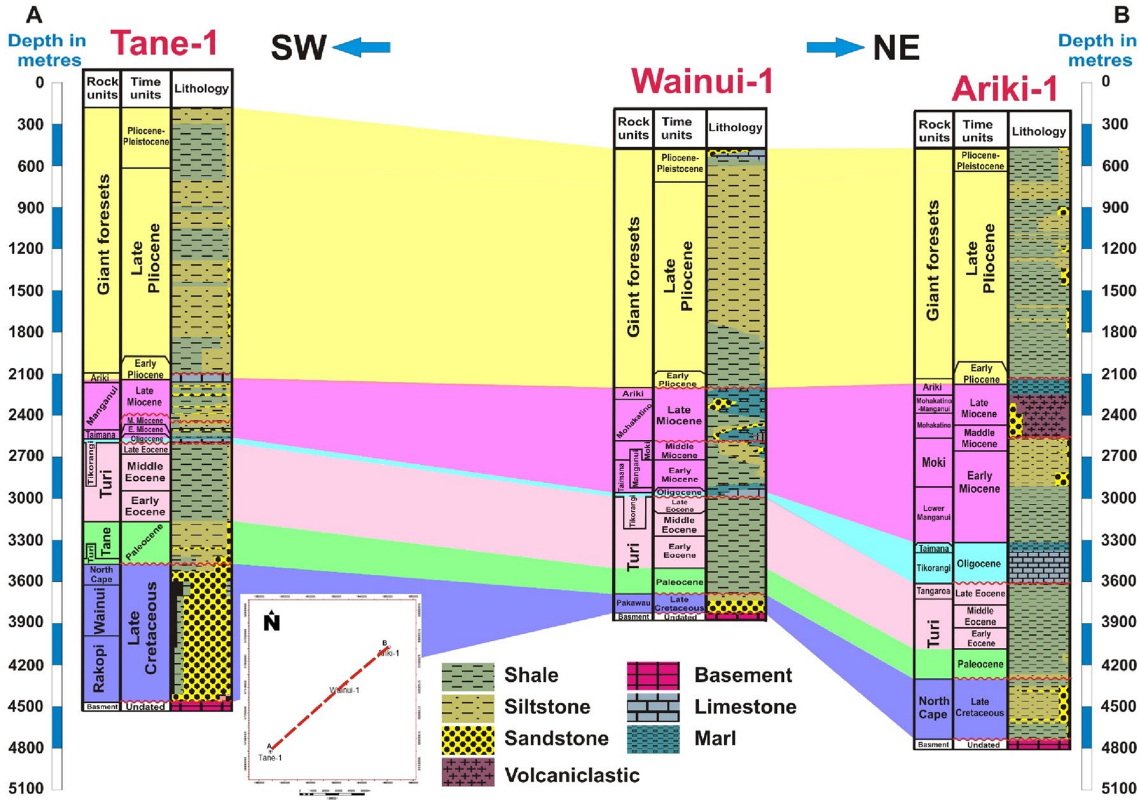

Fig. 6 NE-SW correlation panel illustrating the distribution of the different stratigraphic units encountered in the studied wells

the present-day basin floor and pinch-out toward the shelf (Fig. 5C). In the basinal regions, C3C reflections onlap C3A and C2D facies. The sediments of C3C unit are likely represented by uniform marine shales. Thin (< 300 ms TWT), parallel, continuous high- to medium-amplitude reflections (C3D) onlap the C3B facies near the shelf and downlap onto the C3C in the basinal regions. C3D sediments are thickening near the present-day slope where it attains its maximum thickness of ~ 275 ms TWT.

The sediments of C3D unit are interpreted as being deposited during the maximum sea level rise and therefore comprise a condensed section of marine and organic-rich shales. C3 transgressive megasequence was ended by the deposition of C3E unit that was likely accumulated during highstand systems tract phase. C3E consists of parallel, semi-continuous, medium- to high-amplitude reflections which are widespread throughout the basin. C3E reflections downlap onto C3C unit in the basinal regions where its thickness decreases despite the remarkable increase in seismic amplitude (Fig. 5C, D). C3E sediments comprise marine shales however turbiditic sandstones were likely accumulated in the basinal areas. C3 sequence is represented by the sediments of North Cape Formation which consists of marine sandstones, siltstones and shales intercalated with coal seams that were deposited in a continental shelf depositional environment (Fig. 6). In the eastern part of the present day shelf (Ariki-1 region), C3 facies are represented by C3D, C3E facies that downlap onto the basement rocks (Fig. 5C, D). Westwards, preserved C2 and C3 facies are recorded in Tane-1 well region where the clinoforms reflections of the Taranaki Delta (Rakopi Fm) are followed by the homogeneous medium-amplitude marine facies of C3D sequence.

Paleogene

Extensive shelf conditions prevailed during the deposition of C2 and C3 Cretaceous sequences continued during Early Paleogene. The rate of accommodation space creation likely controlled the thickness and type of the Paleocene and Eocene sediments. Rate of subsidence of the New Zealand land mass exceeded the sediment supply and therefore retrograding Paleocene and Eocene successions were accumulated within an accommodation space of less than 500 m. The Paleocene sequence (P1) displays a uniform seismic facies comprising low-amplitude and semi-transparent reflections with almost constant thickness ranging between 100 and 200 ms TWT on the present-day shelf and slope (Fig. 5C, D). P1 sequence thickens gradually basinwards to a maximum thickness of approximately

500 ms TWT near the Paleocene shelf break and then thins again to less than 100 ms basinwards. The top Paleocene is a uniform surface, however, it is locally drapped over several small channels (~2 km width, Fig. 5C). P1 facies likely comprise marine mudstones and siltstones with sub-marine incised-channel systems, infilled by parallel, high-amplitude and reflectivity reflections onlapping the channel margins. The channels likely contain coarser sediments than those accumulated in the surrounding regions. The high-reflectivity of P1 channel-fill facies may either suggest the presence of hydrocarbons or coarse-grained, porous channel lag deposits (Fig. 5C).

Eocene sequence (P2) displays similar seismic characteristics to P1 comprising semi-transparent, very-low amplitude and reflectivity reflections however it lacks any channel systems. P2 thins basinwards and attains a maximum thickness of approximately 1000 ms TWT near the present-day Taranaki shelf. The seismic characteristics of P2 reflect a homogeneous marine fine-grained clastics analogue to those of the Paleocene. Below the Paleocene shelf edge, P2 thins to approximately 100 ms TWT and the seismic facies change into high-amplitude, semi-parallel reflections typifying a variation in sedimentary facies basinwards likely from clastic to carbonate deposition (Fig. 5C, D). Top Eocene reflector is uniform and is marked by medium- to high-amplitude reflector suggesting sudden change in sedimentary facies. In the eastern part of the present day shelf (Ariki-1 region), P1 and P2 sequences include well-bedded, continuous, low- to medium-amplitude seismic reflections (Fig. 5C). P1 and P2 sediments are represented by homogenous marine mudstones sediments of Turi Formation. Westward in Tane-1 region, P1 is thicker than P2 and both comprise low- to medium-amplitude, parallel and semi-continuous reflections (Fig. 5C). P2 reflections display better continuity than P1. In Tane-1 well, P1 and P2 sequences constitute a retrograding transgressive sedimentary pattern consisting of basal siltstones changing upward into marine mudstones (Fig. 6). Oligocene sequence (P3) consists of continuous, parallel, high- to medium-amplitude reflections. P3 has uniform thin (< 100 ms TWT) thickness throughout the entire basin. It is relatively thinner in the western (Tane-1 well) than in the eastern region (Ariki-1 well) (Fig. 6). P2-P3 boundary is marked by an increase in the acoustic impedance and seismic amplitude. The Oligocene sedimentary facies are represented by carbonate facies reflecting marine deposition coupled with minimal rate of sediment supply. The carbonate rocks of P3 sequence were deposited during a period of high sea level, however, they are probably shallower than the open marine mudstones of P1 and P2 sequences. Therefore, we interpret the Oligocene carbonate as high-stand systems tract facies accumulated after the transgressive facies P1 and P2 sequences.

Sedimentary facies analysis and paleoenvironmental interpretation

Upper cretaceous sequence

In the studied wells (Tane-1, Wainui-1 and Ariki-1), the upper Cetaceous sequence comprises early and late upper Cretaceous Rakopi and North Cape Formation, respectively (Fig. 6). The Rakopi Formation correlates with the progradational C2 sequence, whereas North Cape Formation coincides with the transgressive facies of C3 sequence. The overall thickness of C2 and C3 sequences decreases eastwards and the sediments of Rakopi Formation were only observed in Tane-1 well region (Fig. 6). The analysed side-wall core and cutting samples from Rakopi Formation reveal its sandstone composition interbedded with carbonaceous mudstones and minor coals. The sandstones are stacked in a coarsening-upward sedimentary package with an upward increase in bed thickness and decrease in the mudstone and coal interbeds. The seismic characteristics of C2 sequence (high-amplitude prograding clinoforms) and the corresponding sedimentary facies, both suggest deposition in a prograding delta where the coals and carbonaceous mudstones represent the swamp facies and the coarsening up sandstones represent the distributary channel deposits. This interpretation is supported by the occurrence of palynofloras in the coal seams characterizing a continental depositional environment. Foraminifera are absent; pollen and spore assemblages reflect deltaic and coastal marine environments.

The sediments of C3 sequence were drilled in all the studied wells and are represented by North Cape Formation. In the western part of the present-day shelf (Tane-1 well), North Cape Formation consists of interbedded sandstones, shales and siltstones with thin coal interbeds and carbonaceous mudstones. The sediments are stacked in several progradational coarsening- and thickening-upward sedimentary packages. Eastwards (Ariki-1 well), the sediments of North Cape Formation are also stacked in a coarsening-upward pattern with a vertical change in sedimentary facies from shale- to sand-dominated succession. North Cape sediments contain scarce Foraminifera, however the occurrence of some dinoflagellates in some intervals may reflect marine influence during the deposition.

Sedimentary core samples retrieved from the uppermost part of North Cape Formation in Tane-1 well are characteristic of several sedimentary lithofacies that were accumulated in variable depositional conditions (Table 1). The cored interval typified the deposition of the upper part of North Cape-Formation in a fluvio-deltaic environment. Three main sedimentary facies associations (FA) were observed from the core samples:

Table 1 Characteristics of the sedimentary lithofacies interpreted in the cored intervals within the upper part of the Cretaceous sedimentary succession in Tane-1 well

Sedimentary lithofacies	Characteristics	Depositional processes
Crossbedded sandstone (LF 1)	Light grey, medium-grained sandstones with planar low-angle, and locally slumped cross-beds. Bed thickness is in the range of several centimeters up to few decimeters. Rip-up clasts and mud chips are occasionally observed	High energy deposition from unidirectional traction flows
Heterolithic sandstone/siltstone (LF 2)	Light to dark grey fine to very fine-grained sandstones interlaminated with siltstones and occasionally mudstones. The sandstones are highly-argillaceous. The sediments are slightly bioturbated. The beds range in thickness from several centimeters to decimeters. Thin (~5 cm) lenticular sandstone beds are observed and are occasionally associated with mud drapes	Deposition by low energy tidal currents in coastal-marine environment
Laminated mudstone/siltstone (LF 3)	Dark grey to brown, slightly-fissile mudstones intercalated with siltstones and occasionally very fine-grained sandstones. Planar pinstripe to vague laminations are the main sedimentary structures. Mottling caused by bioturbation is present in the siltstones and very fine-grained sand intervals. However, disruption of sedimentary structures by bioturbation is minor. The beds range in thickness from few to several centimeters	Deposition from suspension in low energy environment
Massive sandstone (LF4)	Medium to coarse-grained, light grey sandstones with no observed sedimentary structures. Bioturbation is absent. Sandstone beds range in thickness from few to several centimeters. Mudstone and siltstone interbeds are absent. Rip- up are locally observed	High energy deposition
Planar and cross-laminated sandstone (LF 5)	Medium to dark grey, fine to very fine-grained sandstones interlaminated with siltstones and locally mudstones. Parallel planar and cross laminae are the main sedimentary structures. The sandstone beds are thin (< 10 cm) and have both gradational bases and tops. The sandstones are slightly bioturbated	Deposition from suspension load in low energy, quite conditions
Ripple cross-laminated sandstone (LF 6)	Medium to dark grey, fine to very fine-grained sandstones, occasionally interlaminated with siltstones and mudstones. Current ripples, climbing ripples and ripple drift laminations are the sedimentary structures observed. Laminae are picked out by carbonaceous debris and clayey material. Slight bioturbation is present. Bed thickness is on the range of few decimeters	Deposition by low energy tidal currents in shallow marine settings
Carbonaceous shale and coal (LF 7)	Dark brown to dull black, massive to banded and thinly- laminated carbonaceous to highly-carbonaceous shale interbedded with coal streaks (< 10 cm). The coal streaks generally take a tabular form and aligned with the bedding planes. Root traces and carbonaceous plant remains are common observed features	Poorly drained, vegetated peat-forming backswamps.

1) Delta-plain distributary channel facies (FA 1) consists of a sharp-based interval of cross-bedded (LF 1) and massive sandstones (LF 4) changing upward into argillaceous planar and cross-laminated sandstones (LF5) (Fig. 7A). The sharp base is mantled by rip-up clasts and mud chips. FA 1 sediments overlie a carbonaceous,

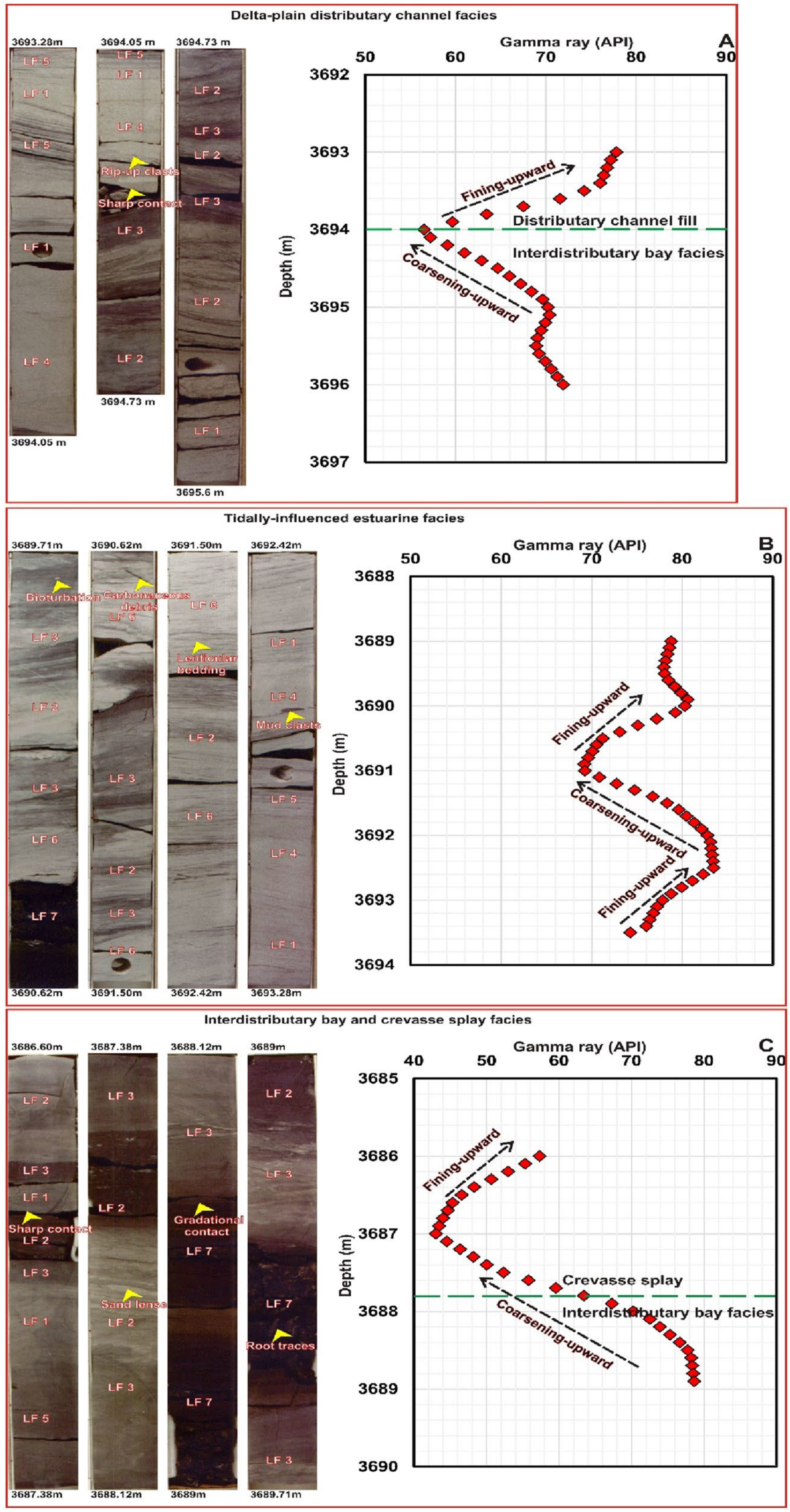

Fig. 7 Core photographs of the studied core interval in the upper part of the Cretaceous succession in Tane-1 well showing the sedimentary lithofacies and their corresponding gamma ray patterns

muddy-rich interval made of massive and laminated mudstones and siltstones with thin sandstone interbeds which likely represent the delta-plain interdistributary bay or crevasse splay facies. FA 1 sandstones are stacked in a fining-upward trend clearly visible from the core and on the gamma ray log pattern (Fig. 7A). The sharp base of the FA 1 sandstones as well as the overall upward decrease in the grain size suggest in channel deposition with decreasing energy of the depositing current (Orton and Reading 1993; Miall 1996; Ainsworth et al. 2011). The sedimentary features in the base FA 1 sandstones are typical for those deposited by traction currents and change upward into suspension deposition suggesting their accumulation in a non-marine river-dominated channels. This further supported by the absence of bioturbation and the non-calcareous nature of the succession. Occurrence of FA 1 sandstones above the carbonaceous-rich mudstone interval supports the interpretation of their accumulation in a subaerial delta-plain environment.

2) Tidally-influenced estuarine facies (FA 2) comprises very fine to fine-grained interval of argillaceous sandstones (LF 2, LF 5, LF 6 and LF7) interlaminated with mudstones and siltstones (LF 3). The sediments are stacked in a successive fining and coarsening-upward patterns (Fig. 7B). Current ripples, climbing ripples and ripple drift laminations are the most common sedimentary structures. Characteristic sedimentary structures comprise heterolithic centimetre-scale wave to lenticular bedding with flat lenses commonly intercalated with mud drapes and mud couplet. The sandstones are slightly bioturbated with tiny *Planolites* and *Chondrites*. The upward increase in heterolithic sediments, first appearance of bioturbation and common occurrence of mud drapes and ripple laminations suggest tidal and marine influence of the sedimentation. Wave and lenticular bedding associated with flat lenses and mud drapes point deposition in a shallow intertidal environment (e.g. Van den berg et al. 2007; MacEachern and Bann 2008; Vakarelov et al. 2012).

3) Interdistributary bay and crevasse splay facies (FA 3) consists of muddy-rich interval locally interbedded with cross-bedded sandstone (LF 1), heterolithic sandstone/siltstone (LF 2) and planar and cross-laminated sandstone (LF 5). The muddy-rich interval constitutes highly-cabonaceous shale and coal seams (LF 7) (Fig. 7C). The carbonaceous shales are rich in root traces typifying their deposition in subaerial continental conditions likely in the delta plain interdistributary bay environment (e.g. Wilhelmsson 1999). This is further supported by the general lack of marine bioturbations and the presence of coals streaks which reflect peat accumulation in a vegetated backswamp environment (e.g. Steel and Dalland 1978; Hansen 2004). The sandstone and siltstone interbeds (LF 1, LF 2, and LF 5) are stacked the deposits of crevasse splay. Festoon crossbedding and vague parallel and cross-laminations are the common sedimentary structures within the crevasse splay sediments. The crossbedded sandstone beds display sharp contacts and often grade upward into argillaceous, fine-grained LF 2 and LF 5 sediments. Occurrence of root traces and carbonaceous woody materials associated with LF 2 sediments reflect accumulation in a subaerial vegetated environment. Crossbedded sandstone grading into argillaceous fine-materials of LF5 suggest gradual decrease in the flow energy and change from traction to suspension sedimentation in a crevasse splay or crevasse channel environment (e.g. Farrell 2001; Burns et al. 2017; Lepre 2017).

Paleocene sequence

The sediments of the Paleocene sequence are represented by the shales of the Lower Turi Formation which are observed in all the studied wells (Fig. 6). The Lower Turi shales are massive and are occasionally intercalated with thin layers of siltstones, very fine-grained sandstones and limestone. A gradual decrease in grain size is observed with upward decrease in the silt and sand intercalations and sand/mud ratio suggesting a deepening upward trend. The Paleocene sediments were deposited in a marine environment as confirmed by the lack of either coal, continental materials or palynomorphs and the occurrence of limestone interbeds as well as marine fossils. The lower part of the Paleocene sequence was likely deposited in an inner neritic environment with upward deepening into a middle neritic setting. This agrees with the benthic foraminiferal assemblage typical of inner to middle neritic conditions such as: *Gaudryina*, *Bulimina*, *Cibicides*, *Oridorsalis*, *Elpidium*, *Buliminella*.

Eocene sequence

Analogue to Paleocene sequence, the sediments of the Eocene sequence consist mainly of massive shales interbedded with limestone. The sandstones and siltstone intercalations are occasionally present, however they are minor if compared with the Paleocene succession. In the studied wells, the early and middle Eocene sediments are represented by the mudstones of the upper part of Turi Formation (Fig. 6). The middle Eocene mudstones contain more frequent limestone interbeds. The sedimentary facies of the late Eocene varies significantly in the studied wells. In Tani-1 and Wainui-1 wells, the late Eocene sediments are represented by the marine mudstones of the upper Turi Formation. In Ariki-1 well, the late Eocene sedimentary facies comprise a ~ 113 m thick, coarsening-upward succession of mudstones and sandstones of the Tangaroa Formation. The Tangaroa sandstones were probably deposited as a large turbidite fan. Generally, the Eocene sediments were deposited in a marine depositional environment likely in a deeper conditions than the underlying Paleocene facies. This is supported by the marine fossils assemblages that are dominated by outer neritic calcareous foraminiferal species in the middle Eocene, such as: *Gaudryina proreussi, plectina quennelli, Valvina bortonica, Lenticulina hampdenensis, Anomalina, visenda, Bulmina bortonica*, and *Cibicides cf. tholus*. During the upper Eocene interval, this assemblage is dominated by more deep forms e.g.: *Cibicides, Rectuvigerina, Euuvigerina*. At the Ariki well, the dominant taxa indicate deep upper bathyal setting (e.g. *Pullenia quinqueloba, Cibicides semiperforatus, Nuttallides truempyi and Oridorsalis umbonatus*).

Oligocene sequence

The Oligocene sequence (P3) in Taranaki region constitutes carbonate facies consisting of planktonic white to light grey foraminiferal micritic and argillaceous lime wackestone grading upward into foraminiferal wackstone-packstone. The sediments of P3 are represented by Tikorangi Formation with a maximum thickness of 146 m in Ariki-1 well (Fig. 6). P3 sediments contain diverse assemblages of benthonic foraminifera, including the simple agglutinating forms *Adercotryma glomeratum, Haplophragmoides,* and *Ammodiscus,* together with *Karreriella, Eggerella* and the more complex *Cyclammina*. Also, the calcareous benthonic forms included; *Cassidulina cuneata, Gyroidina neosoldanii, Pullenia bulloides, Anomalinoides, Gyroidinoides allani* and *Vaginulinopsis interruptus*. These foraminiferal assemblages reveal the deposition of the Oligocene carbonate in a bathyal setting.

Discussion

Depositional sequence stratigraphy

The depositional sequences have been recognized based on the variations in the fossil content (e.g. reworking, variation in foraminiferal assemblage with abrupt changes in planktonic/benthonic contents), lithofacies changes, abrupt variations in gamma ray log pattern and seismic response (Hunt and Tucker 1992; Posamentier and Allen 1999). Three sequence boundaries (SB1, SB2, and SB3) have been observed in the Cretaceous-Paleogene successions encountered in the studied wells (Figs. 8, 9, 10). Most of these sequences are represented by transgressive systems tract (TST) and highstand systems tract (HST), while the lowstand systems tract (LST) are missing. The following is a detailed description of the detected sequences and their bounding surfaces:

The upper cretaceous sequence Sq-1

Sq-1 represents the oldest depositional sequence encountered in the studied wells. The base of this sequence (Sequence boundary, SB1) represents a non-conformity surface above the basement rocks. The basal sediments were initially deposited on an eroded and weathered granitic basement. Sq-1 is represented by prograding clinoforms seismic facies and the gamma ray patterns display successive coarsening-up patterns at the base and fining patterns at

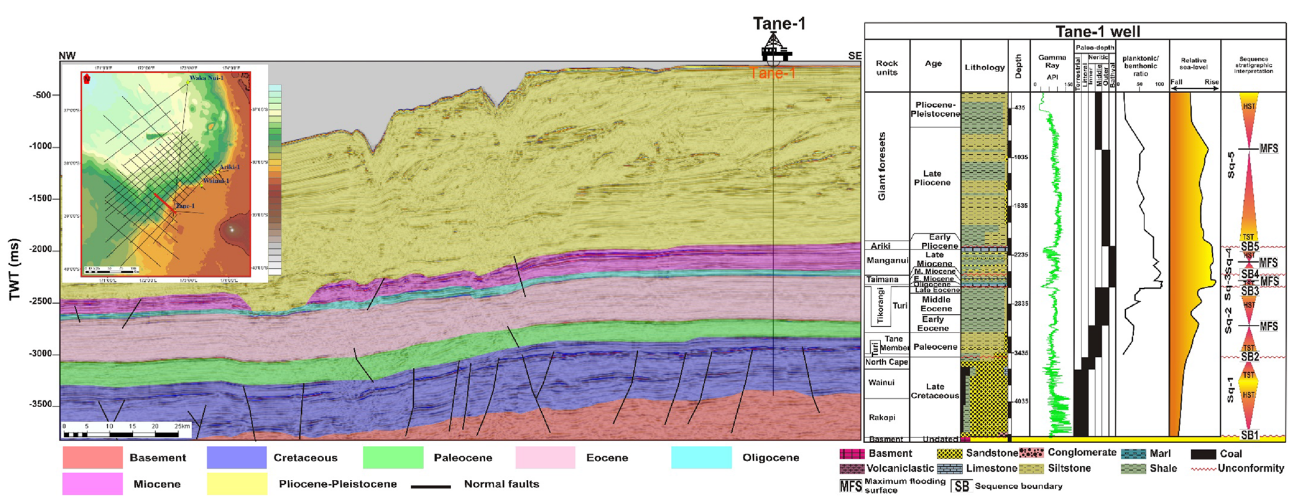

Fig. 8 Interpretation of the different stratigraphic sequences and sequence boundaries encountered in Tane-1 well and correlated with their corresponding seismic facies. Sequence boundaries have been identified based on the variation in lithology, gamma ray pattern and fossil content and planktonic/benthonic forams (P/B ratio)

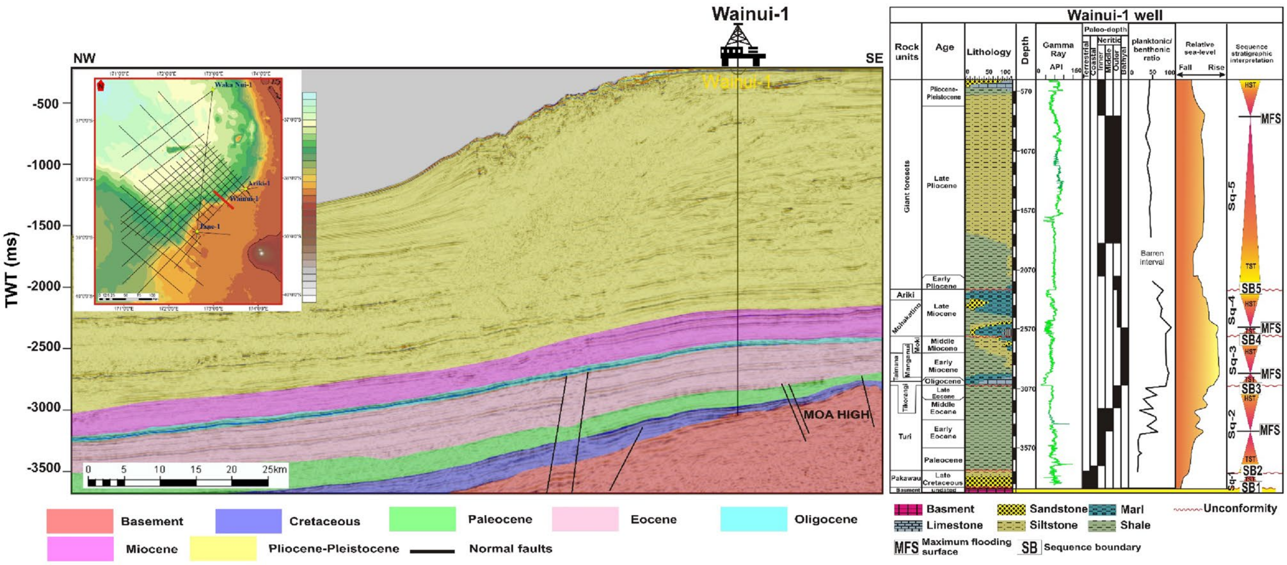

Fig. 9 Interpretation of the different stratigraphic sequences and sequence boundaries encountered in Wainui-1 well and correlated with their corresponding seismic facies. Sequence boundaries have been identified based on the variation in lithology, gamma ray pattern and fossil content and planktonic/benthonic forams (P/B ratio)

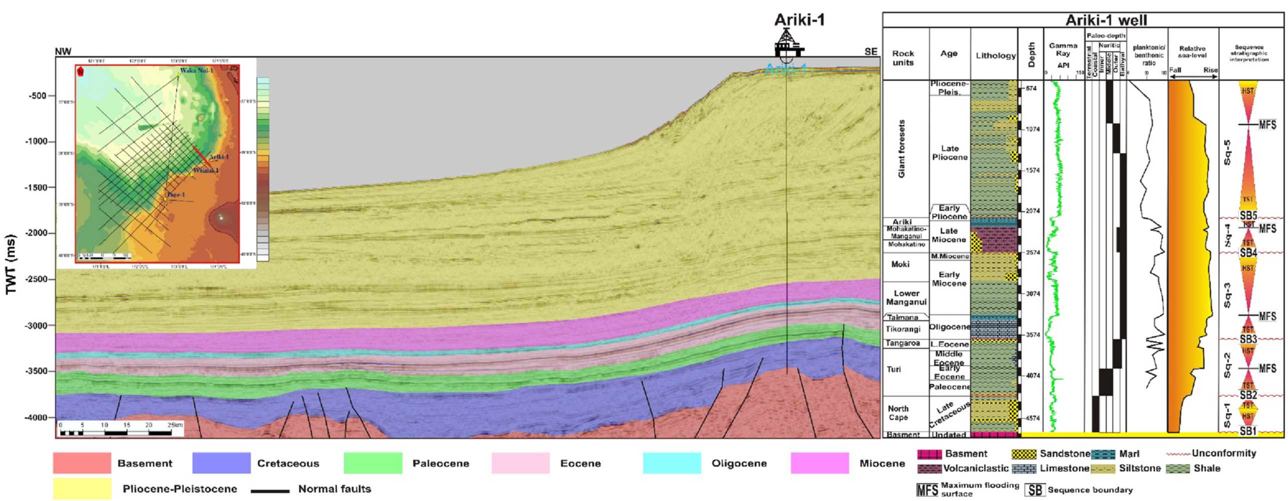

Fig. 10 Interpretation of the different stratigraphic sequences and sequence boundaries encountered in Ariki-1 well and correlated with their corresponding seismic facies. Sequence boundaries have been identified based on the variation in lithology, gamma ray pattern and fossil content and planktonic/benthonic forams (P/B ratio)

the top. At the base, Sq-1 is made up of thick high-energy, prograding fluvial-deltaic sandstones. However, the depositional environment changes upward into estuarine to shallow marine conditions reflecting an upward increase in marine influence (Fig. 11A). The fluvial-deltaic sediments at the base were accumulated during a highstand system tract phase where the sediment supply outpaced the accommodation space allowing the delta and fluvial channels to prograde into the shelf. The basement and faulted highs such as Moa high in Wainui-1 region (Fig. 9) provide a source for the clastic supply prograding onto the shelf (e.g. Norvick et al. 2001; Uruski et al. 2003). The relative sea-level rise and the accumulation of transgressive sedimentary pattern prevailed at the end of Late Cretaceous were tectonically-driven in response to the extensional phase of the Tasman rift (100–80 Ma) (e.g. King et al. 1999; Norvick et al. 2001). The prograded deltaic sediments (Rakopi Formation) corresponds to the Taranaki Delta which is believed as being deposited within the failed back-arc rift of the New Caledonia Basin between 100 and 75 Ma (Sutherland et al. 2001; Uruski et al. 2003; Browne et al. 2007). The sediments of the Taranaki delta are dominated by mudstones and siltstones;

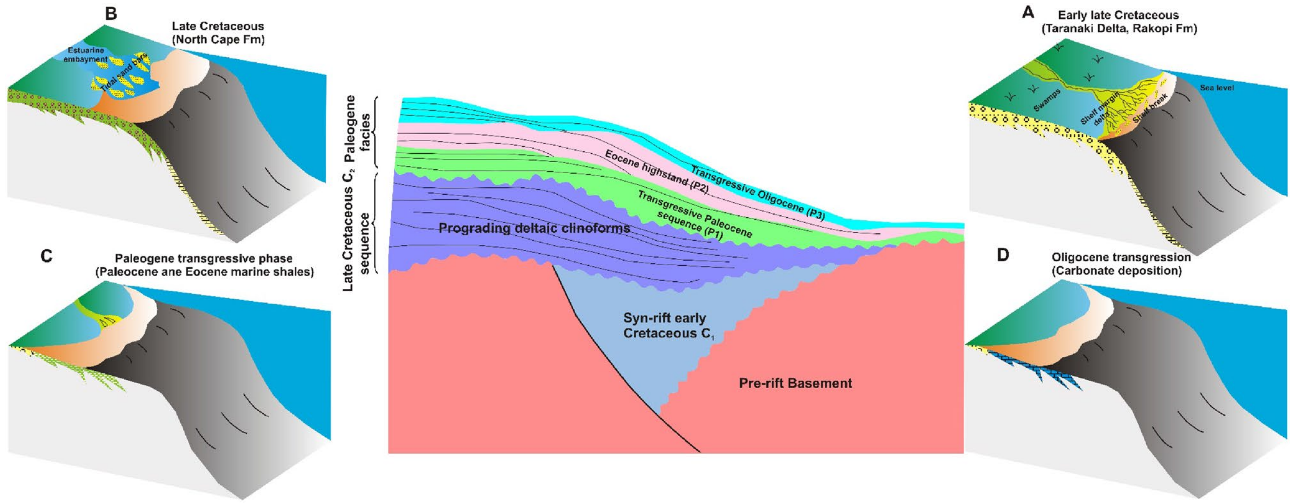

Fig. 11 Schematic cartoon showing the depositional evolution of the studied Cretaceous-Paleogene successions in the northeastern offshore part of Taranaki basin

the sandstones were mostly accumulated within the fluvial and delta distributary channels or in the mouthbars. The occurrence of coal beds occupying the delta-plain implies an ecosystem thrived with plants and vegetation (e.g. Elliott 1978; Miall 2006). This is further supported by the abundant pollen and spores reflecting a flourishing vegetated ecosystems dominated during the deposition of the Taranaki Delta. However, the fairly well-preserved dinoflagellates imply episodic marine conditions.

Transgressive phase prevailed after the deposition of the Taranaki Delta possibly due to accelerated sea level rise in response to thermal subsidence of the New Zealand mini-continent following the extensional rifting of the Tasman Sea (e.g. King et al. 1999; Norvick et al. 2001). The thermal subsidence was accompanied by accelerated sea-level rise coupled with a paramount decrease in the clastic supply thus creating a large accommodation space on the continental shelf where the marine and coastal marine sediments of the North Cape Formation were accumulated with a landward shift of the depositional locus. The sediments of North Cape Formation were accumulated on a nearly flat topography with minimal variations either in the sediment supply or sea-level (Fig. 11B).

The paleocene-eocene sequence Sq-2

Sq-2 is bounded by two sequence boundaries (SB2 and SB3). SB2 is clearly observed at the base of Sq-2 and is marked by an abrupt increase in the gamma ray log values (Figs. 8, 9, 10). On seismic, SB2 is traced between the Cretaceous high-amplitude seismic facies and the overlying low-amplitude, semi-transparent reflections of the Paleocene sediments. SB2 also marks the transition from a coastal to an inner neritic environment. Sq2 comprises two systems tracts TST and HST. The transgressive systems tract (TST) comprises the Paleocene and Early Eocene (Figs. 8, 9, 10) and is characterized by an upward increase in gamma ray and P/B ratios. The benthonic forams assemblage implies an inner to middle neritic environment. The MFS, that separates the TST and HST in this sequence, is characterized by increase in gamma ray values, which indicates the deepest bathymetry, and maximum P/B% (~75%). The HST covers the uppermost part of the Lower Eocene to the Upper Eocene. The transgressive facies are followed by a progradational (HST) succession consisting mainly of shale and limestone interbeds accumulated in a middle-outer neritic environment exhibiting a pronounced decrease in the P/B% (~20–50%). During the deposition of Sq-2, the physiography followed the same pattern of the North Cape Formation, however the locus of the deposition was shifted more landward. Homogeneous marine shales and siltstones were deposited during the Paleocene and Eocene with the deposition in a transgressive marine conditions (Fig. 11C). Thermal subsidence along the Tasman Sea rift continued throughout most of the Paleocene and Eocene and thus keeping accommodation space for the marine sediments to accumulate on the shelf (e.g. King and Trasher 1996; Reilly et al. 2015; Strogen et al. 2017).

The oligocene-middle miocene sequence Sq-3

This depositional sequence constitutes the Oligocene-Middle Miocene succession, it is represented by Tikorangi, Taimana and Lower part of Manganui formations at Tane; Taimana, Manganui and Moki formations at Wainui; and Tikorangi, Taimana and Lower Manganui, and Moki formations at Ariki wells. The Sq3 attains 163 m, 409 m, 104 m

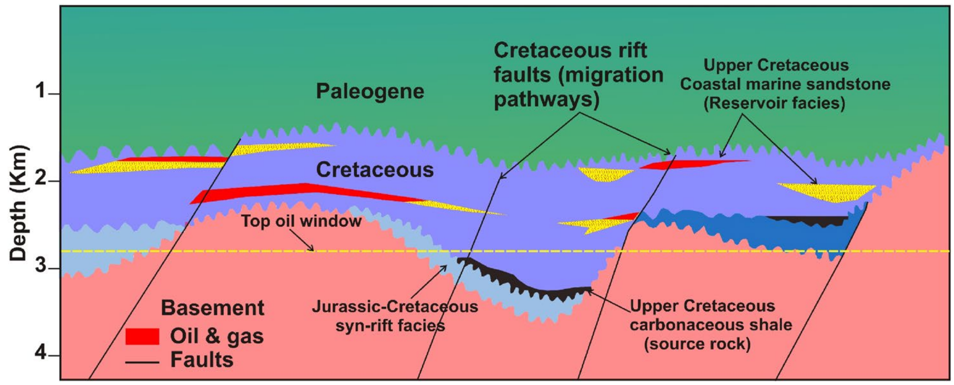

Fig. 12 A simplified sketch of potential source-migration-accumulation hydrocarbon plays within the Cretaceous-Paleogene succession in Taranaki Basin

thick at Tane, Wainui and Ariki wells respectively. The lower boundary of this sequence (SB3) coincides with the Eocene/Oligocene boundary. SB3 documents an abrupt change in lithology from greyish green shales to light grey glauconitic limestone. The transgressive systems tract (TST) of this sequence is marked by the increase in P/B% from ~ 80% at the base to ~ 95% at the top, and the gamma-ray log data are marked by a finning-upward pattern, on the other hand the benthonic assemblage contains bathyal species, these indicate continuous transgression (Figs. 8, 9, 10). The maximum flooding surface (MFS) is placed at the highest positive peak in the P/B% (~ 95%) and coincides with the top of the Oligocene facies.

Oligocene sedimentation is characterized by a major shift in the sedimentation pattern from clastic to carbonate-dominated. This shift is a regional phenomenon following the onset of a new boundary formation between the Australian and pacific plates coupled with development of the Taranaki foredeep along the eastern margin of the basin (Stagpoole and Nicol 2008; Strogen et al. 2014; Reilly et al. 2015). This was accompanied by an abrupt decrease in the rate of sediment supply and clastic input with the development of clean and calm water conditions permitted the carbonate production and deposition (Fig. 11D).

Implications for hydrocarbon exploration

Potential source rock intervals are believed as being associated with late Cretaceous post-rift sediments of C2 sequence (Taranaki Delta or Rakopi Formation). Older Jurassic and early Cretaceous syn-rift facies which host carbonaceous-shales, coals near the shelf and organic-rich marine shales in the deep-water could have been expelled most of hydrocarbons at an early stage (Uruski et al. 2003). Organic-rich facies could be associated with the prograding clinoforms of the C2B unit and probably contain voluminous gas and oil prone kerogen basinwards. The transgressive facies of C2D unit may also contain organic-rich shales basinwards and coal near the present day Taranaki shelf. In addition, coals and carbonaceous-shales in the Rakopi Formation are mostly gas-prone and would generate gas and/or mixed oil and gas. These shales occur in the near shelf foresets and were also carried into the deep-water by the lowstand turbidite fans. These disseminated coals represent potential source rock intervals in the deep water settings. Additionally, the late Cretaceous basin floor fans which represent correlative units to the near-shelf coaly-facies possibly contain voluminous oil prone kerogen that are likely mature and should produce significant amounts of hydrocarbons (Stagpoole et al. 2007; Stagpoole and Nicol 2008).

Potential reservoir targets are associated with the transgressive coastal-marine sandstones of the North Cape Formation and their correlative deep-water turbiditic sandstones. The faults of the early Cretaceous rifting which were locally activated during the progradation of the Taranaki Delta as well as the late Cretaceous faults which extend northward from the present day Taranaki shelf below the slope present the main migration paths from the source rocks into the reservoir intervals (Fig. 12). The Paleogene transgressive marine mudstones (P1-P3 sequences) represent excellent regional seals for the hydrocarbons generated and migrated within the underlying Cretaceous deltaic and coastal-marine facies. Structural and possibly stratigraphic traps exist in the basin. The thickness of the Paleogene sequences is commonly more than 100 m and therefore have a good seal efficiency throughout the entire basin. According to Uruski et al. (2003), the source rock intervals in the Taranaki Delta are currently in the oil window maturity and the present-day oil generation is below 2800 m, whereas the gas window is below 5000 m. The hydrocarbons were likely expulsed from the Cretaceous source rocks during the Eocene–Oligocene, in particular, the Eocene tectonism and activation of the older fault trends promoted the expulsion and migration of the oil and gaseous hydrocarbons which were sealed beneath the Paleogene sedimentary successions.

Conclusive remarks

1. Well and seismic data have been analyzed in order to define the different seismic-stratigraphic sequences and reconstruct the sedimentary evolution of the Cretaceous-Paleogene successions in the north-eastern part of Taranaki Basin, New Zealand.
2. Early Cretaceous syn-rift facies (C1 sequence) were accumulated in the grabens and half-grabens either above crystalline basement or the locally-preserved terrigenous Jurassic facies.
3. The post-rift sequences started with the progradation of the Upper Cretaceous Taranaki Delta succession (C2 sequence) deposited over an extensive continental shelf region.
4. Thermal subsidence along the Tasman Sea rift continued throughout most of the Paleocene and Eocene and thus keeping accommodation space for the marine sediments to accumulate on the continental shelf.
5. End of Paleogene is characterized by a major change in the sedimentation pattern from clastic to carbonate-dominated following the onset of a new plate boundary formation between the Australian and Pacific plates.
6. Voluminous oil and gas-prone kerogen are most probably associated with the prograding facies of the Upper Cretaceous Taranaki Delta and transgressive Paleogene facies, whereas the transgressive sandstones of C3 sequence likely host unexplored potential reservoir intervals.

Acknowledgements The authors are grateful to New Zealand Petroleum & Minerals (a part of the Ministry of Business, Innovation and Employment (MBIE) and GNS Science (Lower Hutt, New Zealand) New Zealand, for kindly providing the subsurface datasets utilized in this study as well as for their permission for publishing.

Funding Open access funding provided by The Science, Technology & Innovation Funding Authority (STDF) in cooperation with The Egyptian Knowledge Bank (EKB).

References

Abdelmaksoud A, Radwan AA (2022) Integrating 3D seismic interpretation, well log analysis and static modelling for characterizing the Late Miocene reservoir, Ngatoro area, New Zealand. Geomech Geophys Geo-Ener Geo-Resour 8(63):1–31. https://doi.org/10.1007/s40948-022-00364-8

Abdelmaksoud A, Amin AT, El-Habaak GH, Ewida HF (2019) Facies and petrophysical modelling of the Upper Bahariya Member in Abu Gharadig oil and gas field, north Western Desert, Egypt. J Afr Ear Sci 149(1):503–516

Ainsworth B, Van der Pal R (2004) Pohokura full field reservoir modelling (cycle 3) part 1: static modelling. Unpublished Petroleum Report 2982, Ministry of Economic Development, Wellington, New Zealand

Ainsworth R, Vakarelov B, Nanson R (2011) Dynamic spatial and temporal prediction of changes in depositional processes on clastic shorelines: toward improved subsurface uncertainty reduction and management. AAPG Bull 95:267–297

Ali M, Abdelhady A, Abdelmaksoud A, Darwish M, Essa MA (2020a) 3D Static modeling and petrographic aspects of the Albian/Cenomanian Reservoir, Komombo Basin. Upper Egypt Nat Resour Res 29(2):1259–1281. https://doi.org/10.1007/s11053-019-09521-5

Ali M, Abdelmaksoud A, Essa MA, Abdelhady A, Darwish M (2020b) 3D Structural, facies and petrophysical modelling of the C Member of Six Hills Formation, Komombo Basin. Upper Egypt Nat Resour Res 29(4):2575–2597

Browne GH, Arnot M, Uruski CI, Field BD, Kennedy E (2007) Reservoir review, PEP 38451, deepwater Taranaki, New Zealand. GNS science consultancy report 2007/49. Prepared for Global Resource Holdings, LLLP

Burns CE, Mountney NP, Hodgson DM, Colombera L (2017) Anatomyand dimensions of fluvial crevasse-splay deposits: examples from the Cretaceous Castelgate Sandstone and Nelsen Formation, Utah. USA Sed Geol 351:21–35

Carter RM (1988) Post-breakup stratigraphy of the Kaikoura Synthem (Cretaceous-Cenozoic), continental margin, southeastern New Zealand. NZ J Geol Geophys 31:405–429

Cook RA, Sutherland R et al (1999) Cretaceous–Cenozoic geology and petroleum systems of the Great South Basin, New Zealand. Institute of Geological & Nuclear Sciences Monograph 20

Elliott T (1978) Deltas. In: Reading H (ed) Sedimentary environments and facies, 2nd edn. Blackwell Scientific Publications, Oxford, pp 113–154

Farrell KM (2001) Geomorphology, facies architecture, and high-resolution, non-marine sequence stratigraphy in avulsion deposits, Cumberland Marshes, Saskatchewan. Sed Geol 139:93–150

Giba M, Nicol A, Walsh JJ (2010) Evolution of faulting and volcanism in a back-arc basin and its implications for subduction processes. Tectonics 29: TC2040. https://doi.org/10.1029/2009TC002634

Hansen JA (2004) Paleogeographic reconstruction of the Firkanten Formation (Paleocene) in Reindalen area. Norgen teknisknaturvitenskaplige universitet, Trondheim, Spitsbergen. M.Sc.

Higgs K, King P, Raine J, Sykes R, Browne G, Crouch E, Baur J (2012) Sequence stratigraphy and controls on reservoir sandstone distribution in an Eocene marginal marine-coastal plain fairway, Taranaki Basin, New Zealand. J Mar Pet Geol 32:110–137

Hunt DW, Tucker M (1992) Stranded parasequences and the forced regressive wedge system tract: deposition during base-level fall. Sed Geol 81:1–9

Isaac MJ, Herzer RH, Brook FJ, Hayward BW (1994) Cretaceous and Cenozoic sedimentary basins of Northland, New Zealand. Institute of Geological & Nuclear Sciences Monograph 8

Kamp PJJ, Vonk AJ et al (2004) Neogene stratigraphic architecture and tectonic evolution of Wanganui, King Country, and eastern Taranaki basins, New Zealand. NZ J Geol Geophys 47:625–644
King PR (2000) Tectonic reconstructions of New Zealand 40 Ma to the present. NZ J Geol Geophys 43:611–638
King PR, Thrasher GP (1996) Cretaceous-Cenozoic geology and petroleum systems of the Taranaki basin, New Zealand. In: Institute of Geological & Nuclear Sciences Monograph, Lower Hutt. 13 (pp 244)
King PR, Naish TR, Browne GH, Field BD, Edbrooke SW (1999) Cretaceous to Recent sedimentary patterns in New Zealand. Institute of Geological and Nuclear Sciences folio series 1, version 1999.1.
King PR, Naish TR, Browne GH, Field BD, Edbrooke SW (2011) Cretaceous to Recent sedimentary patterns in New Zealand. Digitally remastered version. Institute of Geological & Nuclear Sciences Folio Series 1a
Kroger K, Crutchley G, Hill M, Pecher I (2017) Potential for gas hydrate formation at the northwest New Zealand shelf margin: New insights from seismic reflection data and petroleum systems modelling. Mar Petrol Geol 83:215–230
Laird MG, Bradshaw JD (2004) The break-up of a long-term relationship: the Cretaceous separation of New Zealand from Gondwana. Gondwana Res 7:273–286
Laird MG (1992) Cretaceous stratigraphy and evolution of the Marlborough segment of the East Coast region. In: New Zealand Petroleum Conference Proceedings 1991, Ministry for Economic Development, Wellington (pp 89–100)
Laird M (1993) Cretaceous continental rifts: New Zealand region. In: Ballance PF (ed) South Pacific sedimentary basins. Sedimentary basins of the world, 2, Elsevier Science Publishers, Amsterdam (pp 37–49)
Leila M, Yasser A, El Bastawesy M, El Mahmoudi A (2022) Seismic stratigraphy, sedimentary facies analysis and reservoir characteristics of the Middle Jurassic syn-rift sediments in Salam Oil Field, north Western Desert. Egypt Marr Petrol Geol 136:105466. https://doi.org/10.1016/j.marpetgeo.2021.105466
Lepre CJ (2017) Crevasse-splay and associated depositional environments of the hominin-beariong lower Okote Member, Koobi For a Formation (Plio-Pleidstocene0, Kenya. The Depositional Record 3:161–186
MacEachern J, Bann K (2008) The role of ichnology in refining shallow marine facies models: recent advances in models of siliciclastic shallow marine stratigraphy. In: Hampson J, Steel R, Burgess P, Dalrymple R (eds) SEPM Spec. Publ, 90 (pp 73–116)
Miall A (1996) The geology of fluvial deposits: sedimentary facies, basin analysis and petroleum geology. Springer, Berlin Heidelberg, pp 582
Miall AD (2006) The Geology of Fluvial Deposists: Sedimentary Facies, Analysis and Petroleum Geology. Spring-Verlag, New York, pp 582
Mortimer N, Rattenbury MS et al (2014) High-level stratigraphic scheme for New Zealand rocks. NZ J Geol Geophys 57:402–419. https://doi.org/10.1080/00288306.2014.946062
Nazeer A, Abbasi SA, Solangi SH (2016) Sedimentary facies interpretation of Gamma Ray (GR) log as basic well logs in Central and Lower Indus Basin of Pakistan. Geodesy Geodynam 7(6):432–443
Nicol A, Walsh J, Berryman K, Nodder S (2005) Growth of a normal fault by the accumulation of slip over millions of years. J Struct Geol 27:327–342
Nicol A, Mazengarb C, Chanier F, Rait G, Uruski CI, Wallace LM (2007) Tectonic evolution of the active Hikurangi subduction margin, New Zealand, since the Oligocene. Tectonics 26: TC4002. https://doi.org/10.1029/2006TC002090
Norvick MS, Smith MA, Power MR (2001) The plate tectonic evolution of eastern Australasia guided by the stratigraphy of the Gippsland Basin. In: Hill KC, Bernecker T (eds) Eastern Australian Basin Symposium 2001. Petroleum Exploration Society of Australia, Melbourne, pp 15–23
Orton GJ, Reading HG (1993) Variability of deltaic processes in terms of sediment supply, with particular emphasis on grain size. Sedimentology 40(475–512):7
Posamentier H, Allen G (1999) Siliciclastic sequence stratigraphy: concepts and appliocations. SEPM 7 Tulsa. https://doi.org/10.20110/csp.99.07
Radwan AA, Nabawy BS (2022) Hydrocarbon prospectivity of the miocene-pliocene clastic reservoirs, Northern Taranaki basin, New Zealand: integration of petrographic and geophysical studies. J Petrol Expl Prod Tech. https://doi.org/10.1007/s13202-021-01451-4
Radwan AA, Nabawy BS, Abdelmaksoud A, Lashin A (2021) Integrated sedimentological and petrophysical characterization for clastic reservoirs: a case study from New Zealand. J Nat Gas Sci Eng 88:103797
Radwan AA, Nabawy BS, Shihata M, Leila M (2022) Seismic interpretation, reservoir characterization, gas origin and entrapment of the Miocene-Pliocene Mangaa C sandstone, Karewa Gas Field, North Taranaki Basin, New Zealand. Mar Petrol Geol 135:105420. https://doi.org/10.1016/j.marpetgeo.2021.105420
Reilly C, Nicol A, Walsh JJ, Seebeck H (2015) Evolution of faulting and plate boundary deformation in the Southern Taranaki Basin, New Zealand. Tectonophysics 651–652:1–18. https://doi.org/10.1016/j.tecto.2015.02.009
Rider M, Rider MH (2002) Facies, sequences and depositional environments from logs. In: The geological interpretation of well logs, 2nd Ed. Sutherland, Scotland, Rider-French Consulting, (pp 226–238)
Ryan WB, Carbotte SM, Coplan JO, O'Hara S, Melkonian A, Arko R, Weissel RA, Ferrini V, Goodwillie A, Nitsche F, Bonczkowski J (2009) Global multi-resolution topography synthesis. Geochem Geophys Geosyst. https://doi.org/10.1029/2008GC002332
Stagpoole V, Davy B, Wood R (2007) Potential field modelling of deepwater taranaki basin PEP 38451. GNS Science Consultancy Report 2007/24. Prepared for Global Resource Holdings, LLLP
Stagpoole V, Nicol A (2008) Regional structure and kinematic history of a large subduction back thrust: Taranaki Fault, New Zealand. J Geophys Res 113
Steel R, Dalland A (1978) Undersøkelser av den kullførende del av Firkanten Formasjonen (Tertiær) i østlige del av Nordenskiøld land Svalbard, Geologisk Institutt Universitetet i Bergen
Strogen DP, Bland KJ, Nicol A, King PR (2014) Paleogeography of the Taranaki Basin region during the latest Eocene-Early Miocene and implications for the 'total drowning' of Zealandia. NZ J Geol Geophys 57:110–127. https://doi.org/10.1080/00288306
Strogen D, Seebeck H, Nicol A, King P (2017) Two-phase Cretaceous-Paleocene rifting in the Taranaki Basin region, New Zealand; implications for Gondwana break-up. J Geol Soc. https://doi.org/10.1144/jgs2016-160
Sutherland R, King P, Wood R (2001) Tectonic evolution of Cretaceous rift basins in southeastern Australia and New Zealand: implications for exploration risk assessment. PESA Eastern Australasia Basins Symposium 3–13
TGS-NOPEC (2001) Astrolabe Seismic Survey. Ministry of Economic Development, New Zealand. Unpublished Petroleum Report PR 2847
Turnbull IM, Uruski CI et al (1993) Cretaceous and Cenozoic sedimentary basins of western Southland, South Island, New Zealand. Institute of Geological & Nuclear Sciences Monograph, 1, Institute of Geological & Nuclear Sciences, Lower Hutt
Uruski CI, Baillie P (2004) Mesozoic evolution of the greater Taranaki Basin and implications for petroleum prospectivity. APPEA J 44:385–395
Uruski CI, Baillie P, Stagpoole VM (2003) Development of the Taranaki Basin and comparisons with the Gippsland Basin: implications for deepwater exploration. APPEA J 43:185–196
Vakarelov BK, Ainsworth R, MacEachern J (2012) Recognition of wave-dominated, tide-influenced shoreline systems in the rock record: variations from a microtidal shoreline model. Sediment Geol 279:23–41

Van den Berg J, Boersma J, Van Gelder A (2007) Diagnostic sedimentary structures of the fluvial-tidal transition zone- evidence from deposits of the Rhine and Meuse. Neth J Geosci 86:306–387

Wilhelmsson JC (1999) Depositional environments and sequence stratigraphy of the coal bearing Todalen Member, Firkanten Formation (Paleocene), Adventdalen, Svalbard [Unpublished Cand. Scient Thesis]: University of Oslo 89

Yasser A, Leila M, El Bastawesy M, El Mahmoudi A (2021) Reservoir heterogeneity analysis and flow unit characteristics of the Upper Cretaceous Bahariya Formation in Salam Field, north Western Desert, Egypt. Arab J Geosci 14:1635.https://doi.org/10.1007/s12517-021-07985-5